

The One Phonon Raman Spectrum of Silicon Nanostructures

Pedro Alfaro, Miguel Cruz, and Chumin Wang

Abstract—Porous silicon is a structurally complex material, in which effects of the pore topology on its physical properties are even controversial. We use the Born potential and the Green's function, both applied to a supercell model, in order to analyze the Raman response and the phonon band structure of porous silicon. In this model, the pores are simulated by empty columns of atoms, in direction [001], produced in a crystalline silicon structure. An advantage of this model is the interconnection between silicon nanocrystals, then, all the states are extended. The results show that the Raman spectra are sensitive to the pore topology. Moreover, a shift of the main Raman peak towards lower frequencies is found, in agreement with experimental data.

Index Terms—Phonons, Raman scattering, silicon nanostructures.

I. INTRODUCTION

THE luminescence observed in nanostructured semiconductors has motivated a great quantity of theoretical and experimental investigations [1], [2], because it has many potential applications in optoelectronics devices [3]. In particular, a uniform layer of porous silicon (PSi) can be obtained from a substrate of crystalline silicon (c-Si) when it is anodized in a solution of hydrofluoric acid with an appropriate current density. This PSi layer consists of a skeleton of c-Si whose typical thickness is of nanometer order. The size, morphology, and distribution of pores vary with the preparation conditions of PSi samples. During the last decade, the scientific community has devoted a great effort to understanding the pore formation mechanism and the origin of its luminescence. However, little attention has been paid to the study of elementary excitations in PSi. For example, the effects of the pore topology on the phonon behavior are still unclear.

Raman scattering is a tool broadly used to investigate vibrational properties of semiconductors. In the particular case of PSi, it has been used to determine the structure type, size, and morphology of the pores, as well as the surface effects on the acoustic bands [4]. In all cases, the experimental data show a shift and a broadening of the main Raman peak toward lower frequency [5]. In this paper, we analyze phonon band structures and Raman response of PSi by means of the Green's function,

the Born potential, including central and not central forces, and a supercell model, in which the pores are dug by removing Si atoms.

II. MODEL

Let us consider an interaction potential (V_{ij}) between nearest neighbor atoms i and j , as given in the Born model [6]

$$V_{ij} = \frac{1}{2}(\alpha - \beta) \{[\mathbf{u}(i) - \mathbf{u}(j)] \cdot \hat{\mathbf{n}}_{ij}\}^2 + \frac{1}{2}\beta [\mathbf{u}(i) - \mathbf{u}(j)]^2 \quad (1)$$

where $\mathbf{u}(i)$ is the displacement of atom i with respect to its equilibrium position, and α and β are, respectively, central and noncentral restoring force constants. The unitary vector $\hat{\mathbf{n}}_{ij}$ indicates the bond direction between i and j atoms. The Dyson equation for the Green's function (\mathbf{G}) can be written as [7]

$$(M\omega^2\mathbf{I} - \Phi)\mathbf{G}(\omega) = \mathbf{I} \quad (2)$$

where M is the atomic mass of Si, \mathbf{I} stands the matrix identity, and Φ is the dynamic matrix, whose elements are given by

$$\Phi_{\mu\mu'}(i, j) = \frac{\partial^2 V_{ij}}{\partial u_{\mu}(i) \partial u_{\mu'}(j)} \quad (3)$$

with $\mu, \mu' = x, y, \text{ or } z$.

If axis z is chosen along $\hat{\mathbf{n}}_{ij}$, the Born interaction matrix (ϕ) has a simple form

$$\phi = - \begin{pmatrix} \beta & 0 & 0 \\ 0 & \beta & 0 \\ 0 & 0 & \alpha \end{pmatrix}. \quad (4)$$

However, ϕ should be expressed in coordinates of the solid, i.e., it is necessary to make proper rotations of ϕ . For tetrahedral structures, the positions of four nearest neighbor atoms around a central atom located at (0,0,0) are $R_1 = (1, 1, 1)a/4$, $R_2 = (-1, -1, 1)a/4$, $R_3 = (-1, 1, -1)a/4$, and $R_4 = (1, -1, -1)a/4$. Hence, the four corresponding interaction matrices ϕ can be written as

$$\phi_1 = - \begin{pmatrix} (\alpha + 2\beta)/3 & (\alpha - \beta)/3 & (\alpha - \beta)/3 \\ (\alpha - \beta)/3 & (\alpha + 2\beta)/3 & (\alpha - \beta)/3 \\ (\alpha - \beta)/3 & (\alpha - \beta)/3 & (\alpha + 2\beta)/3 \end{pmatrix} \quad (5)$$

$$\phi_2 = - \begin{pmatrix} (\alpha + 2\beta)/3 & (\alpha - \beta)/3 & (\beta - \alpha)/3 \\ (\alpha - \beta)/3 & (\alpha + 2\beta)/3 & (\beta - \alpha)/3 \\ (\beta - \alpha)/3 & (\beta - \alpha)/3 & (\alpha + 2\beta)/3 \end{pmatrix} \quad (6)$$

$$\phi_3 = - \begin{pmatrix} (\alpha + 2\beta)/3 & (\beta - \alpha)/3 & (\alpha - \beta)/3 \\ (\beta - \alpha)/3 & (\alpha + 2\beta)/3 & (\beta - \alpha)/3 \\ (\alpha - \beta)/3 & (\beta - \alpha)/3 & (\alpha + 2\beta)/3 \end{pmatrix} \quad (7)$$

Manuscript received January 14, 2006; revised June 9, 2006. This work was supported in part by CGPI-IPN-2005303, CONACyT-49291, and DGAPA-IN110305. Calculations were carried out in Bakliz of the DGSCA-UNAM. The review of this paper was arranged by Associate Editor R. Lake.

P. Alfaro and M. Cruz are with the Instituto Politécnico Nacional, ESIME-Culhuacán, México 04430, México (e-mail: irisson@servidor.unam.mx).

C. Wang is with the Instituto de Investigación en Materiales, Universidad Nacional Autónoma de México, México 04510, México (e-mail: chumin@servidor.unam.mx).

Digital Object Identifier 10.1109/TNANO.2006.881273

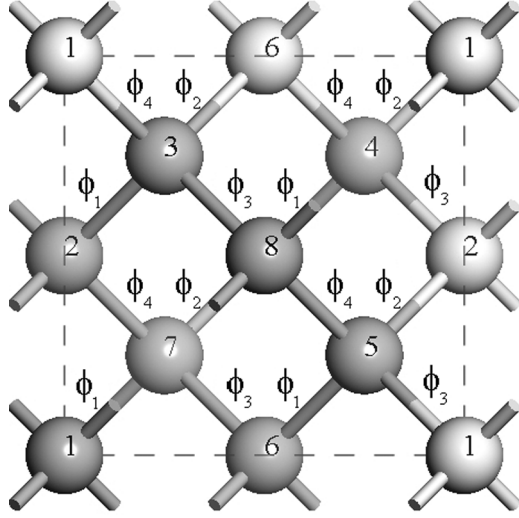


Fig. 1. Supercell of eight-atom Si viewed in [001] direction, used to model crystalline silicon. Force constants of tetrahedral connections are given by matrix, ϕ_1 , ϕ_2 , ϕ_3 , and ϕ_4 .

and

$$\phi_4 = - \begin{pmatrix} (\alpha + 2\beta)/3 & (\beta - \alpha)/3 & (\beta - \alpha)/3 \\ (\beta - \alpha)/3 & (\alpha + 2\beta)/3 & (\alpha - \beta)/3 \\ (\beta - \alpha)/3 & (\alpha - \beta)/3 & (\alpha + 2\beta)/3 \end{pmatrix}. \quad (8)$$

For the tetrahedral symmetry, it is easy to prove that

$$\phi_s = \phi_1 + \phi_2 + \phi_3 + \phi_4 = -\frac{4}{3}(\alpha - 2\beta)I. \quad (9)$$

The Fourier transform of Φ can be written as in the equation shown at the bottom of the page, where the equilibrium positions of atoms i and j are, respectively, written as $\vec{l} + \vec{b}$ and $\vec{l}' + \vec{b}'$, where \vec{l} , \vec{l}' are the unit cells and \vec{b} , \vec{b}' the positions inside these cells. The changes of phase related to the phonon wave vector (\mathbf{q}) are given by $F_1 = e^{i\mathbf{q}\cdot R_1}$, $F_2 = e^{i\mathbf{q}\cdot R_2}$, $F_3 = e^{i\mathbf{q}\cdot R_3}$, and $F_4 = e^{i\mathbf{q}\cdot R_4}$.

Fig. 1 shows a cubic supercell with sides of $a = 5.431 \text{ \AA}$, containing eight Si atoms, where the four interaction matrices ϕ_1 , ϕ_2 , ϕ_3 , and ϕ_4 are indicated. The pores can be produced when we remove columns of atoms in the supercell of c-Si along the [001] crystalline direction. The pore topology is determined by eliminating different atoms in the supercell. In this paper, we use supercells of 32-atoms built by putting in the plane X-Y four

eight-atom supercells illustrated in Fig. 1. Hence, 32-atom supercells have a tetragonal structure with parameters $a_x = a_y = 2a$ and $a_z = a$.

On the other hand, the Raman scattering in solids is a complex process that involves photons, electrons, and phonons. Therefore, any microscopic theory should consider the dynamic correlation between atomic movements and changes in the local polarization of the bonds around each atom [8].

Since the wave vector of the visible light is much smaller than the first Brillouin zone, the momentum conservation law only allows the participation of vibrational modes around the Γ point ($\mathbf{q} = 0$).

Within the local polarization model of bonds and the linear response theory, the Raman spectrum $[R(\omega)]$ can be calculated by [8], [9]

$$R(\omega) \propto \omega \text{Im} \sum_{\mu, \mu'} \sum_{i, j} (-1)^{i-j} G_{\mu\mu'}(i, j, \omega) \quad (10)$$

where i and j are the atoms index, and the Green's function $[G_{\mu\mu'}(i, j, \omega)]$ is defined in (2).

Once we have chosen the supercell and the interaction model, we are ready to calculate the phonon band structure and the Raman response for pores with different morphology.

III. RESULTS

Fig. 2(a) and (b) shows the c-Si phonon band structure and Raman response, obtained from a base of 2 Si atoms in an fcc unit cell, as illustrated in the inset of Fig. 2(b). The numeric calculations were done by using the Born model parameters $\alpha = 120.3 \text{ Nm}^{-1}$ and $\beta = 23.5 \text{ Nm}^{-1}$, which are obtained by comparing the theoretical phonon dispersion relationship with the inelastic neutron scattering data [10]. In Fig. 2, it can be observed that the Raman response of c-Si is located at 519.3 cm^{-1} , which corresponds to the highest frequency of optical modes.

In Fig. 3(a) and (b), we show, respectively, the phonon band structure and Raman response of PSi with a porosity of 12.5%, and its atomic configuration is schematically drawn in the inset. The pores are produced by removing columns of Si atoms along [001] crystalline direction. Observe that there are several peaks in the Raman response spectrum and the highest frequency peak has a shift toward lower energy in comparison with the c-Si case. This increased number of active Raman modes at the Γ point, as shown in Fig. 3(a), is directly related to the employment of

$$D_{\mu\mu'}(\vec{b}\vec{b}'|\vec{q}) = \sum_{\vec{l}\vec{l}'} \Phi_{\mu\mu'}(\vec{l}\vec{b}, \vec{l}'\vec{b}') e^{i\vec{q}\cdot(\vec{l}-\vec{l}')} = \begin{pmatrix} \phi_s & 0 & F_4\phi_4 & F_2\phi_2 & F_3\phi_3 & 0 & F_1\phi_1 & 0 \\ 0 & \phi_s & F_1\phi_1 & F_3\phi_3 & F_2\phi_2 & 0 & F_4\phi_4 & 0 \\ F_4^*\phi_4 & F_1^*\phi_1 & \phi_s & 0 & 0 & F_2^*\phi_2 & 0 & F_3^*\phi_3 \\ F_2^*\phi_2 & F_3^*\phi_3 & 0 & \phi_s & 0 & F_4^*\phi_4 & 0 & F_1^*\phi_1 \\ F_3^*\phi_3 & F_2^*\phi_2 & 0 & 0 & \phi_s & F_1^*\phi_1 & 0 & F_4^*\phi_4 \\ 0 & 0 & F_2\phi_2 & F_4\phi_4 & F_1\phi_1 & \phi_s & F_3\phi_3 & 0 \\ F_1^*\phi_1 & F_4^*\phi_4 & 0 & 0 & 0 & F_3^*\phi_3 & \phi_s & F_2^*\phi_2 \\ 0 & 0 & F_3\phi_3 & F_1\phi_1 & F_4\phi_4 & 0 & F_2\phi_2 & \phi_s \end{pmatrix}$$

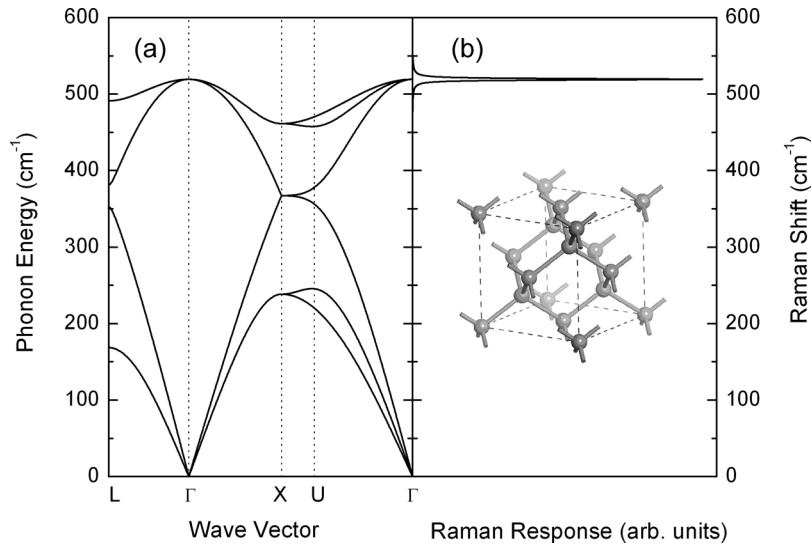


Fig. 2. (a) Phonon bands structure and (b) Raman response of c-Si obtained from fcc lattice with base of two Si atoms, as illustrated in inset.

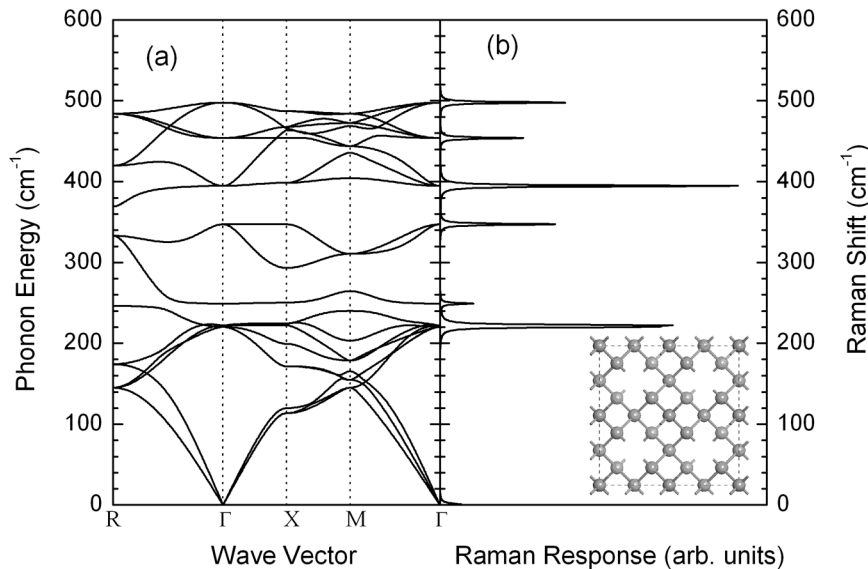


Fig. 3. (a) Phonon band structure and (b) Raman response for PSi with 12.5% porosity, when Si atom is removed from eight-atom supercell.

the supercell technique and its consequent folding of the first Brillouin zone in the reciprocal space. But, in a real PSi sample, there is no supercell periodicity. Therefore, it is not expected that we have such a large number of active Raman modes in real PSi. On the other hand, there is a shift of the highest frequency Raman peak, from 519.3 cm^{-1} for c-Si to 497.9 cm^{-1} for PSi, as shown in Fig. 3(b). This shift can be interpreted as a smoother curvature of optical phonon wavefunctions due to the absence of certain atoms when the pores are introduced. Also, such a shift can be understood within the quantum confinement theory as the following. The highest frequency optical mode is reached when the wave length of the modulation is infinity and the presence of pores introduce extra nodes, located at pore surfaces, which determine the available longest phonon modulation wave length. For the case of 12.5% porosity, the separation of these nodes is about 5.76 \AA (see inset of Fig. 3). Within the fully confined phonon model, this separation of nodes leads to

a new highest frequency optical mode at 495.7 cm^{-1} , obtained from the band structure of Fig. 2(a). However, in our case, such confinement is only partial, since there are interconnections between quantum wires [11], which produce a slight higher frequency optical mode.

In Fig. 4(a) and (b), numerical results of the phonon band structure and the Raman response are, respectively, shown for a PSi sample with the same porosity as in Fig. 3, except that in this case we remove four neighbor Si atoms in a 32-atom supercell, as schematically illustrated in the inset of Fig. 4. Notice that the highest frequency Raman peak is located at 512.2 cm^{-1} , which is produced by a less intense quantum confinement caused by a pore separation of 11.52 \AA instead of 5.76 \AA for the case of Fig. 3. Again, there is an even larger number of Raman peaks in Fig. 4(b), which is a consequence of a larger supercell. They would be eliminated if a random pore structure were introduced, as discussed.

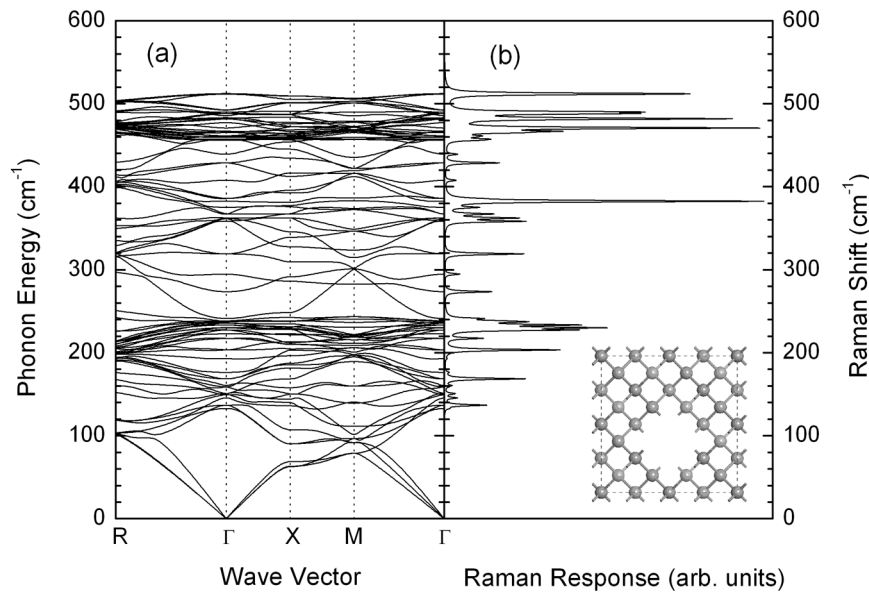


Fig. 4. (a) Phonon band structure and (b) Raman response for PSi with same porosity as in Fig. 3 and different pore distribution.

IV. CONCLUSION

The results show a relocation of the highest frequency Raman peak toward lower energies when the pores are introduced, in qualitative agreement with experimental data. The origin of this relocation could be thought as a consequence of the extra nodes found at the pore surface, an effect similar to the quantum confinement, although the phonon wave functions are extended. Also, the results have clearly shown that the Raman response depends not only on the porosity but also on the pore distribution. It is important to mention that the calculations have been performed within a supercell model, which has an inherent defect of emphasizing the periodicity in the pore distribution, which is a lack in real PSi samples. Therefore, a random pore distribution factor should be introduced to improve the supercell model [12], such as was done by means of the coherent potential approximation. This improvement is currently in progress.

REFERENCES

- [1] D. Lockwood, *Light Emission in Silicon from Physics to Devices*. London, U.K.: Academic, 1998.
- [2] A. G. Cullis, L. T. Canham, and P. D. J. Calcott, "The structural and luminescence properties of porous silicon," *J. Appl. Phys.*, vol. 82, p. 909, 1997.
- [3] T. Yoshida, N. Suzuki, T. Makino, and Y. Yamada, "Near-IR LEDs fabricated with monodispersed nanocrystallite Si," *Solid State Technol.*, vol. 45, p. 41, 2002.
- [4] H. Tanino, A. Kuprin, H. Deai, and N. Koshida, "Raman study of free-standing porous silicon," *Phys. Rev. B, Condens. Matter*, vol. 53, p. 1937, 1996.
- [5] D. J. Lockwood, M. H. Kuok, S. C. Ng, and Z. L. Rang, "Surface and guided acoustic phonons in porous silicon," *Phys. Rev. B, Condens. Matter*, vol. 60, p. 8878, 1999.
- [6] A. S. Carriço, R. J. Elliott, and R. A. Barrio, "Modelling the Raman spectrum of the amorphous-crystal Si system," *J. Phys. C*, vol. 19, p. 1113, 1986.
- [7] R. J. Elliott, J. A. Krumhansl, and P. L. Leath, "The theory and properties of randomly disordered crystals and related physical systems," *Rev. Mod. Phys.*, vol. 46, p. 465, 1974.
- [8] R. Alben, D. Weaire, J. E. Smith, and M. H. Brodsky, "Vibrational properties of amorphous Si and Ge," *Phys. Rev. B, Condens. Matter*, vol. 11, p. 2275, 1975.
- [9] C. Wang and R. A. Barrio, "Theory of the Raman response in Fibonacci superlattices," *Phys. Rev. Lett.*, vol. 61, p. 191, 1988.

- [10] J. L. Martins and A. Zunger, *Handbook of Interatomic Potential Semiconductors*, vol. III, V. J.B. Torres and A. M. Stoneham, Eds., Atomic Energy Research Establishment Harwell, U.K., Nov. 1985, p. Si.7.
- [11] M. Cruz, C. Wang, M. R. Beltrán, and J. Tagüeña-Martínez, "Morphological effects on the electronic band structure of porous silicon," *Phys. Rev. B, Condens. Matter*, vol. 53, p. 3827, 1996.
- [12] M. Cruz, M. R. Beltrán, C. Wang, J. Tagüeña-Martínez, and Y. G. Rubo, "Supercell approach to the optical properties of porous silicon," *Phys. Rev. B, Condens. Matter*, vol. 59, p. 15381, 1999.



Pedro Alfaro received the B.S. degree in communications and electronic engineering from ESIME Culhuacan, National Polytechnic Institute, Mexico. Currently, he is pursuing the Ph.D. degree at the same institute, studying the dynamical and electronic properties of silicon and germanium nanostructures.



Miguel Cruz received the B.S. degree in physics and the M.S. and Ph.D. degrees in materials science, all from the National Autonomous University, Mexico.

He joined the National Polytechnic Institute, where he is now a Professor and the Coordinator of the Masters of Engineering program in energy systems. His research interests include the electronic and optical properties of nanomaterials.



Chumin Wang received the B.S., M.S., and Ph.D. degrees in physics from the National Autonomous University (UNAM), Mexico.

He was a Postdoctoral Associate at the Department of Physics, University of California, Berkeley, from 1993 to 1994. He is currently a Researcher at the Materials Research Institute, UNAM. His research interests include strongly correlated electron systems and elementary excitations in quasi-crystals as well as in porous materials.